SUPPORTING INFORMATION

Assessing the Role of Counterion in Gold Catalyzed Dearomatization of Indoles with Allenamides by NMR Studies

Luca Rocchigiani,[†] *Minqiang Jia,*[‡] *Marco Bandini*[*,‡] *and Alceo Macchioni*[*,†,#]

[†]Department of Chemistry, Biology and Biotechnology, University of Perugia and CIRCC, Via Elce di sotto, 8, I-06123 Perugia, Italy

[‡]Department of Chemistry "G. Ciamician", Alma Mater Studiorum – University of Bologna, Via Selmi 2, I-40126 Bologna, Italy

[#]Istituto di Scienze e Tecnologie Molecolari del CNR (CNR-ISTM), c/o Department of Chemistry, Biology and Biotechnology, University of Perugia, I-06123, Perugia, Italy

Email: marco.bandini@unibo.it, alceo.macchioni@unipg.it

1. General procedures – page S2
2. Relevant NMR spectra – page S4
3. *In situ* NMR catalytic experiments – page S13

1. General procedures

Complex **1**Cl was synthesized following known method[1] and complex **1**TFA was obtained via halogen metathesis reactions (**1**Cl + AgTFA) as previously described.[2]
Samples of **1**OTf were generated *in situ* within a screw cap NMR tube, by reacting the suitable amount of **1**Cl with an excess of AgOTf in methylene chloride-d_2. 15 minutes after mixing, the solution was filtered into another screw cap NMR tube in order to remove the excess of AgOTf and formed AgCl. Quantitative ^{1}H and ^{19}F NMR spectra were performed to assess the purity of the complex (>90%).
Unless specified, NMR samples were prepared in open air by using methylene chloride-d_2 dried over CaH_2. Experiments in exclusion of water and oxygen were performed by loading the suitable amount of solids within a J-Young NMR tube, which was interfaced to an high vacuum Schlenk line ($<10^{-5}$ Torr) and dried overnight. Then, dry methylene chloride-d_2 was condensed into the NMR tube at 77K and kept at low temperature before inserting the sample into the NMR probe.
1D- and 2D-NMR spectra were measured on a Bruker Avance III HD 400 spectrometer equipped with a ^{1}H,BB smartprobe. Referencing is relative to solvents (^{1}H and ^{13}C), CCl_3F (^{19}F) and 85% H_3PO_4 (^{31}P). ^{1}H NOESY NMR experiments were acquired by using the PFG pulse sequence version;[3] $^{19}F,^{1}H$ HOESY NMR experiments were acquired by using the standard four-pulse sequence or its modified version.[4] The number of transients and the number of data points were chosen according to the sample concentration and to the desired final digital resolution. Semi-quantitative spectra were acquired with 1s relaxation delay and 800ms mixing time.
^{1}H PGSE (Pulsed Field gradient Spin Echo) NMR measurements were performed by using a double stimulated sequence, containing 3 spoil gradients and longitudinal encode-decode (dstegp3s1d), on a Bruker Avance III HD NMR spectrometer equipped with a ^{1}H,BB smartprobe, at 298K without spinning. The dependence of the resonance intensity on a constant waiting time and on a varied gradient strength G is described as:

$$\ln\frac{I}{I_0} = (\gamma\delta)^2 D_t\left(\Delta - \frac{\delta}{3}\right)G^2$$

where I is the intensity of the observed spin echo, I_0 is the intensity of the spin echo in the absence of gradient, D_t is the self-diffusion coefficient, Δ is the delay between the midpoints of the gradients, δ is the length of the gradient pulse and γ is the magnetogyric ratio. The shape of the gradients was rectangular, their length δ was 4-5 ms and their strength was varied during the experiments. Spectra were acquired for 64k points with a spectral width of 6000 Hz and processed with a line broadening of 1.0. The semi-logarithmic plots of $\ln(I/I_0)$ versus G^2 were fitted by using a standard linear regression algorithm. Different values of Δ, G, and number of transients were used for different samples. Hydrodynamic data were derived by using solvent as internal standard as reported elsewhere.[5]

1TFA – ^{1}H NMR (400.13 MHz, methylene chloride-d_2, 298K) δ7.52 (m, H2 $P(OR)_3$), 7.49 (dd, $J_{H,H}$=8.6 and 1.5 Hz, H5 $P(OR)_3$), 7.23 (dd, $J_{H,H}$=8.6 and 2.5 Hz, H4 $P(OR)_3$), 1.49 (s, *t*-Bu^1 $P(OR)_3$), 1.33 ppm (s, *t*-Bu^2 $P(OR)_3$). ^{19}F NMR (376.5 MHz, methylene chloride-d_2, 298K) δ–74.0 ppm (s, TFA). ^{31}P{^{1}H} NMR (150.0 MHz, methylene chloride-d_2, 298K) δ88.6 ppm (s, $P(OR)_3$).

1OTf – ^{1}H NMR (400.13 MHz, methylene chloride-d_2, 298K) δ7.52 (m, H2 $P(OR)_3$), 7.44 (d, $J_{H,H}$=8.6, H5 $P(OR)_3$), 7.23 (dd, $J_{H,H}$=8.6 and 2.4 Hz, H4 $P(OR)_3$), 1.49 (s, *t*-Bu^1 $P(OR)_3$), 1.33 ppm (s, *t*-Bu^2 $P(OR)_3$). ^{19}F NMR (376.5 MHz, methylene chloride-d_2, 298K) δ–77.7 ppm (s, TFA). ^{31}P{^{1}H} NMR (150.0 MHz, methylene chloride-d_2, 298K) δ85.4 ppm (s, $P(OR)_3$).

2. Relevant NMR spectra

2.1 1TFA + 2

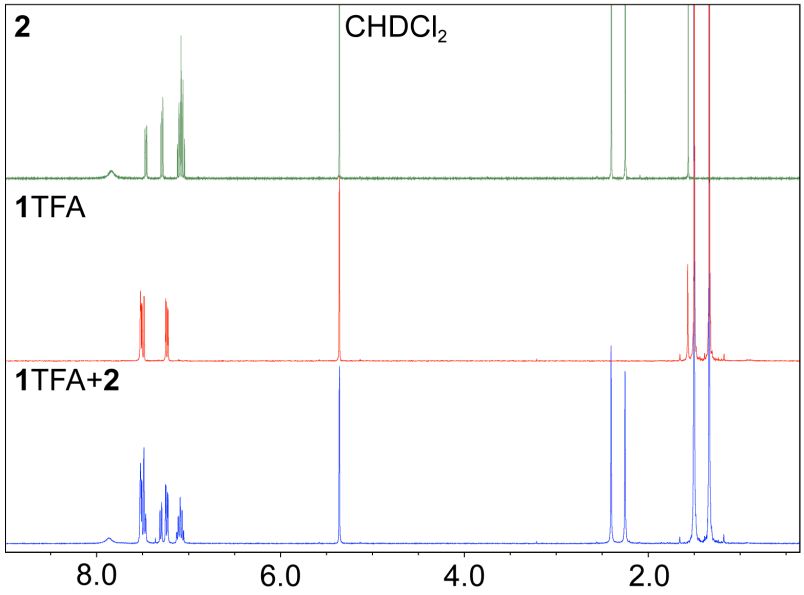

Figure S1. Comparison between ^{1}H NMR spectra of **1**TFA, **2** and their mixture in anhydrous methylene chloride-d_2 at 298K.

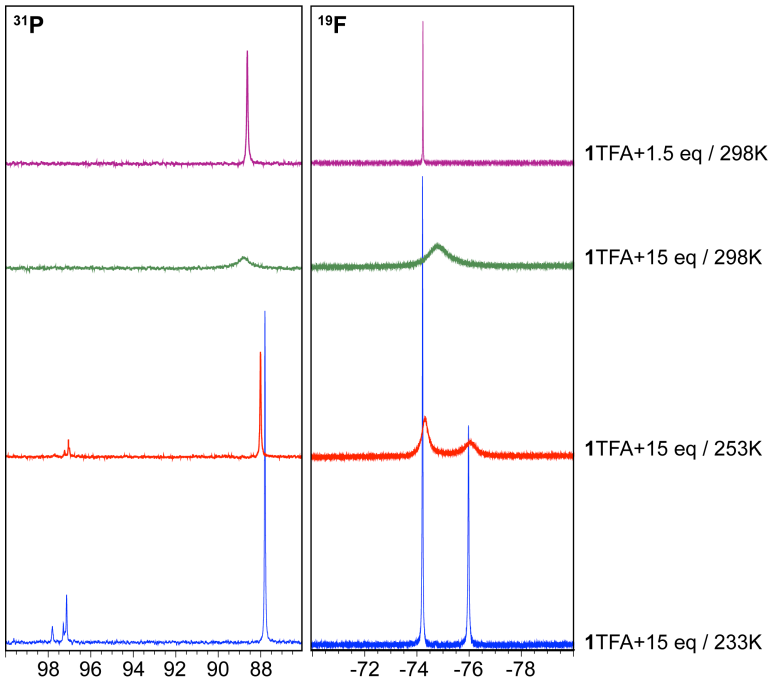

Figure S2. ^{31}P{^{1}H} and ^{19}F NMR spectra obtained after the addition of different equivalents of **2** to **1**TFA at different temperatures in anhydrous methylene chloride-d_2.

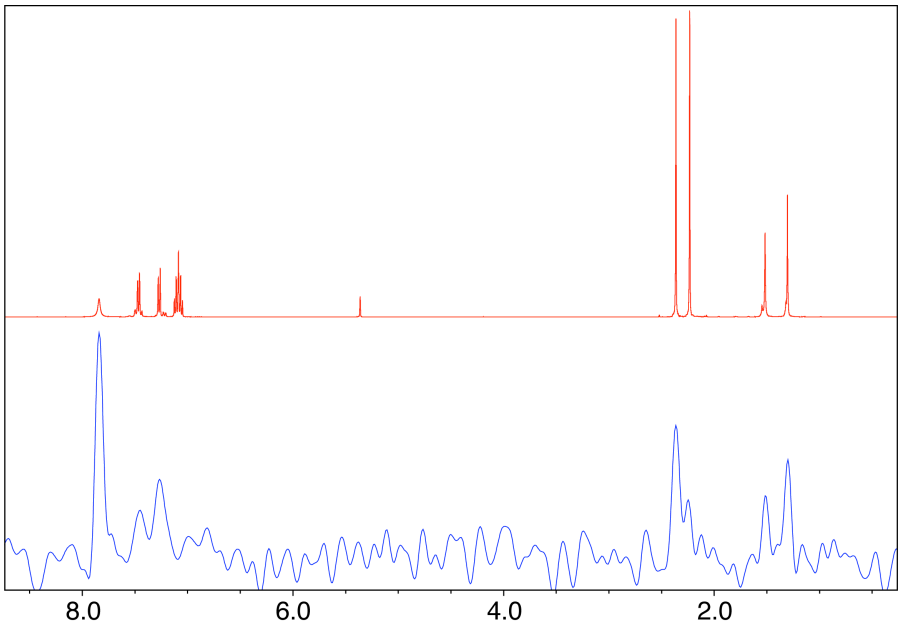

Figure S3. Comparison between ^{1}H and trace at δ_F= – 72.2 ppm of the ^{19}F, ^{1}H HOESY NMR spectra of a mixture containing **1**TFA and 15 equivalents of **2** at 233 K in anhydrous methylene chloride-d_2.

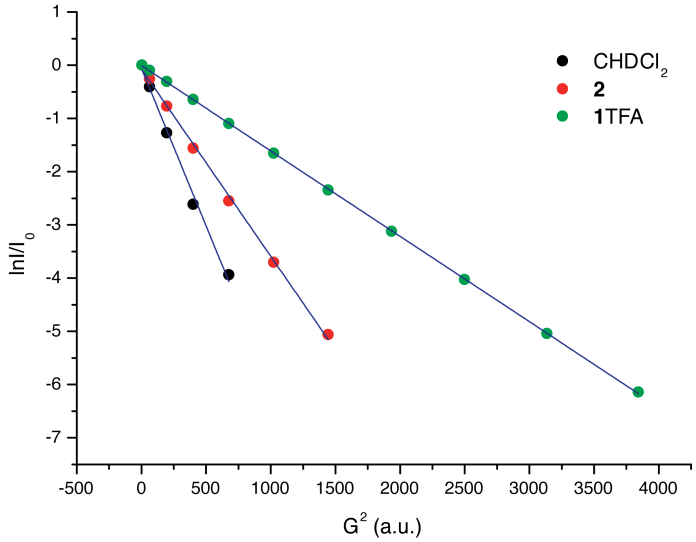

Figure S4. lnI/I$_0$ vs. G^2 plot for a mixture containing **1**TFA and 15 equivalents of **2** at 298 K in anhydrous methylene chloride-d_2. Data analysis gave an hydrodynamic volume value of 170 A^3 for **2** and 998 A^3 for **1**TFA, suggesting that the two species have a low tendency to interact at room temperature.

2.2 1OTf + 2

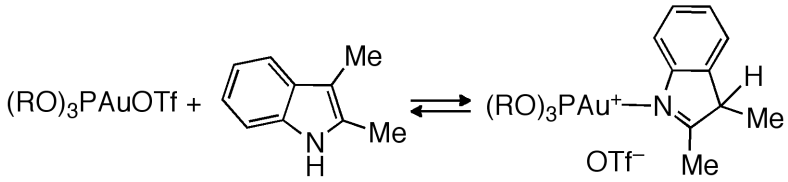

Scheme S1. Reaction between **1**OTf and **2**.

Selected ^{1}H NMR resonances (400.13 MHz, methylene chloride-d_2, 298K) δ7.58 (m, P(OR)$_3$), 7.31 (buried under **2**, P(OR)$_3$), 7.27 (buried under **2**, P(OR)$_3$), 4.00 (q, $J_{H,H}$=7.9 Hz, H3), 2.46 (s, H1), 1.54 (d, $J_{H,H}$=7.9 Hz, H2), 1.53 (s, P(OR)$_3$), 1.35 ppm (s, P(OR)$_3$). Selected ^{13}C{^{1}H} NMR resonances (100.55 MHz, methylene chloride-d_2, 298K) δ51.0 (s, C3), 30.9 (s, P(OR)$_3$), 30.2 (s, P(OR)$_3$), 19.2 (s, C1), 14.2 ppm (s, C2). ^{19}F NMR (376.5 MHz, methylene chloride-d_2, 298K) δ–78.7 ppm (s, OTf$^-$). ^{31}P{^{1}H} NMR (150.0 MHz, methylene chloride-d_2, 298K) δ97.3 ppm (s, P(OR)$_3$).

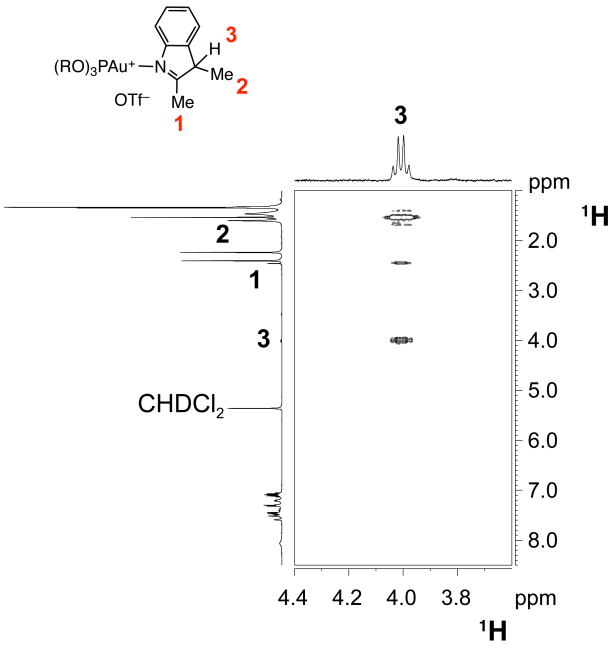

Figure S5. A section of the ^{1}H COSY NMR spectrum obtained after mixing **1**OTf and 2 equivalents of **2** in methylene chloride-d_2 showing scalar coupling of H3 with H2 and H1.

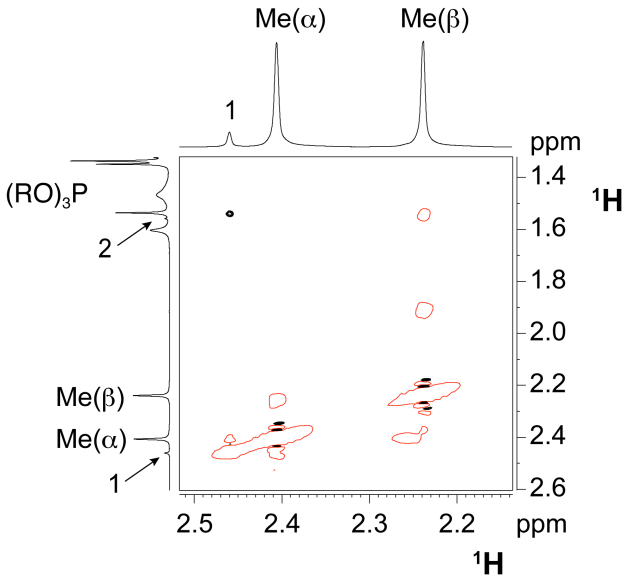

Figure S6. A section of the ^{1}H NOESY NMR spectrum obtained after mixing **1**OTf and 2 equivalents of **2** in methylene chloride-d_2 showing chemical exchange of H1 and H2 with Me(α) and Me(β) of **2**.

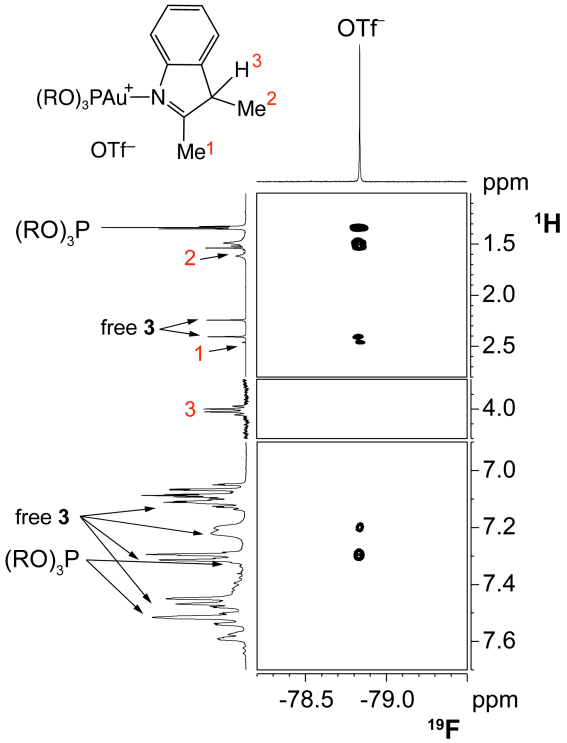

Figure S7. ^{19}F,^{1}H HOESY NMR spectrum obtained after mixing **1**OTf and 2 equivalents of **2** in methylene chloride-d_2 at 298K.

2.3 1TFA + 3

a) Reactivity in the presence of traces of water:

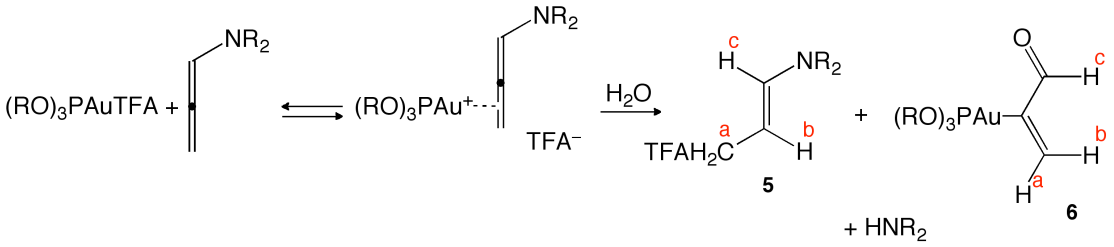

Scheme S2. Proposed deactivation pathway of gold-allene species in the presence of H_2O leading to anion transfer to substrate, allene hydrolysis and [Au(I)]-acrolein.

Selected ^{1}H NMR resonances (400.13 MHz, methylene chloride-d_2, 253K) δ9.84 (d, $J_{H,P}$=15.6 Hz, Hc of **6**), 7.64 (d, $J_{H,H}$=8.4 Hz, Ts of HNR_2), 7.55 (d, $J_{H,H}$=8.4 Hz, Ts of **5**), 7.48 (m, Hc of **5** + $(RO)_3P$), 7.35 (d, $J_{H,H}$=8.4 Hz, Ts of **5**), 7.55 (d, $J_{H,H}$=8.4 Hz, Ts of **5**), 7.28 (d, $J_{H,H}$=8.4 Hz, Ts of HNR_2), 7.21 (m, $(RO)_3P$), 7.14 (m, Ph of HNR_2), 7.07 (m, $(RO)_3P$), 6.95 (m, Ph of **5**), 6.70 (s, NH of HNR_2), 6.55 (dd, $J_{P,H}$=21.9 Hz, $J_{H,H}$=3.2 Hz, Hb of **6**), 6.35 (dd, $J_{P,H}$=10.0 Hz, $J_{H,H}$=3.2 Hz, Ha of **6**), 4.79 (d, $J_{H,H}$=8.0 Hz, Ha of **5**), 4.43 (dt, $J_{H,H}$=13.8 Hz, $J_{H,H}$=8.0 Hz, Hb of **5**), 2.47 (s, Ts of **5**), 2.39 (s, Ts of HNR_2), 1.47 (s, $(RO)_3P$), 1.29 ppm (s, $(RO)_3P$). Selected $^{13}C\{^{1}H\}$ NMR resonances (100.55 MHz, methylene chloride-d_2, 253K) δ203.1 (d, $J_{P,C}$=4.2 Hz, Cc of **6**), 149.7 (s, Ca/b of **6**), 145.8 (s, Cc of **5**), 100.8 (s, Cb of **5**), 67.5 (s, Ca of **5**), 31.1 (s, $(RO)_3P$), 29.9 (s, $(RO)_3P$), 21.6 ppm (s, Ts of **5** and Ts of HNR_2). ^{19}F NMR (376.5 MHz, methylene chloride-d_2, 253K) δ–75.3 ppm (s, TFA of **5**). $^{31}P\{^{1}H\}$ NMR (150.0 MHz, methylene chloride-d_2, 253K) δ141.2 (s, $P(OR)_3$), 119.6 ppm (s, $(RO)_3PAuP(OR)_3^{+}$).

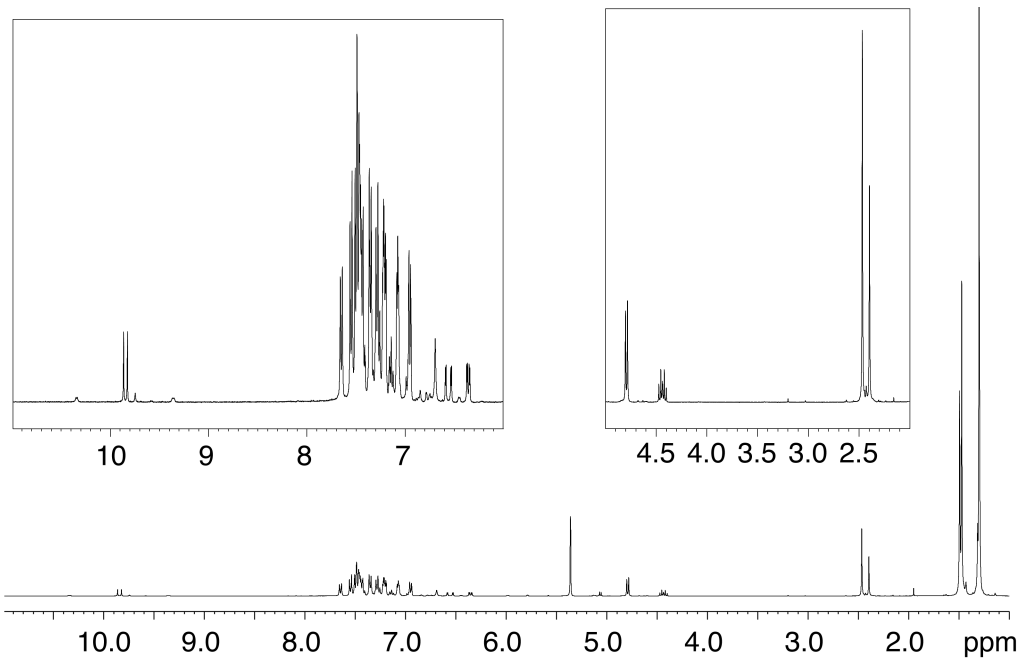

Figure S8. ^{1}H NMR spectrum obtained after mixing **1**TFA with 1.2 equivalents of **3** in methylene chloride-d_2 in the presence of water traces (T = 253K).

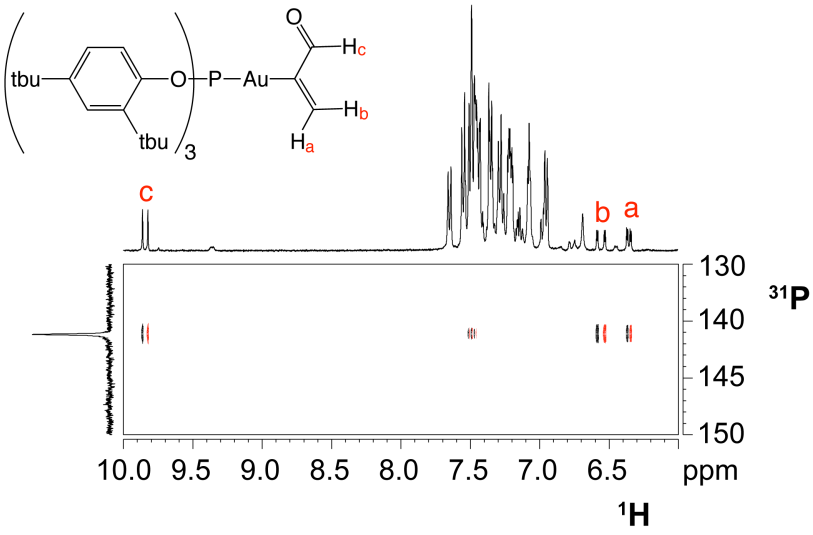

Figure S9. A section of the $^{1}H,^{31}P$ phase sensitive HMBC NMR spectrum obtained after mixing **1**TFA with 1.2 equivalents of **3** in methylene chloride-d_2 in the presence of water traces (T = 253K).

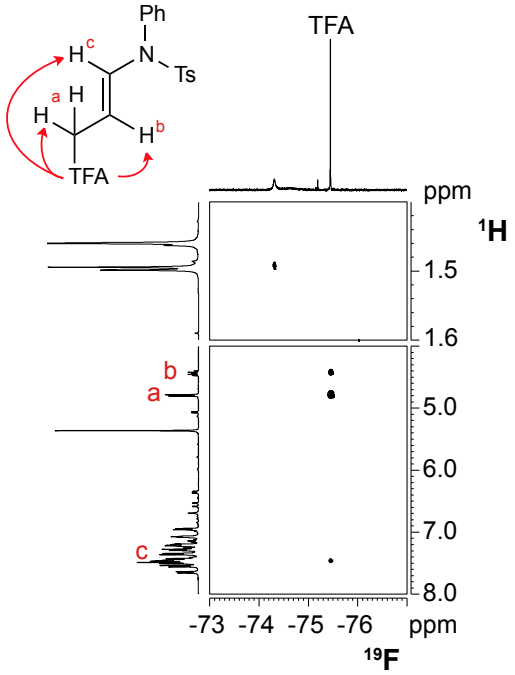

Figure S10. $^{19}F,^{1}H$ HOESY NMR spectrum obtained after mixing **1**TFA with 1.2 equivalents of **3** in methylene chloride-d_2 in the presence of water traces (T = 253K). Red arrows denote NOEs.

b) Reactivity in dry conditions:

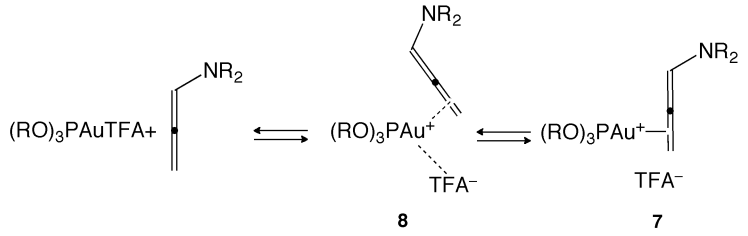

Scheme S3. Proposed reactivity between **1**TFA and **3** under rigorous dry conditions in methylene chloride at 233 K.

Selected ^{1}H NMR resonances (400.13 MHz, methylene chloride-d_2, 233K) δ7.52 (d, $J_{H,H}$=8.3 Hz, Ts of free **3**), 7.47 (m, $(RO)_3P$ of **1**TFA), 7.42 (m, $(RO)_3P$ of **7**/**8**), 7.34 (d, $J_{H,H}$=8.3 Hz, Ts of free **3**), 7.29 (brd, Ts of coordinated **3**), 7.20 (m, $(RO)_3P$ of **1**TFA+**7**/**8**), 7.15 (t, $J_{H,H}$=6.3 Hz, CH of free **3**), 6.72 (brd, Ph of coordinated **3**), 5.05 (d, $J_{H,H}$=6.3 Hz, CH_2 of free **3**), 4.83 (brd, CH_2 of coordinated **3**), 2.45 (s, Ts of free **3**), 2.43 (s, Ts of coordinated **3**), 1.49 (s, $(RO)_3P$ of **1**TFA), 1.42 (s, $(RO)_3P$ of **7**/**8**), 1.28 (s, $(RO)_3P$ of **1**TFA), 1.27 ppm (s, $(RO)_3P$ of **7**/**8**). Selected $^{13}C\{^{1}H\}$ NMR resonances (100.55 MHz, methylene chloride-d_2, 233K) δ129.8 (s, Ph of coordinated **3**), 125.2 (s, $(RO)_3P$ of **7**/**8**), 123.8 (s, Ts of coordinated **3**), 77.5 (s, CH_2 of coordinated **3**), 31.2 (s, $(RO)_3P$ of **7**/**8**), 30.1 (s, $(RO)_3P$ of **7**/**8**), 21.8 ppm (s, Ts of coordinated **3**). ^{19}F NMR (376.5 MHz, methylene chloride-d_2, 233K) δ−73.5 (brs, TFA **8**), −74.3 (s, **1**TFA), −75.0 ppm (s, TFA **7**). $^{31}P\{^{1}H\}$ NMR (150.0 MHz, methylene chloride-d_2, 233K) δ139.6 (s, $P(OR)_3$ of **7**), 130.1 (s, $P(OR)_3$ of **8**), 87.8 ppm (s, **1**TFA).

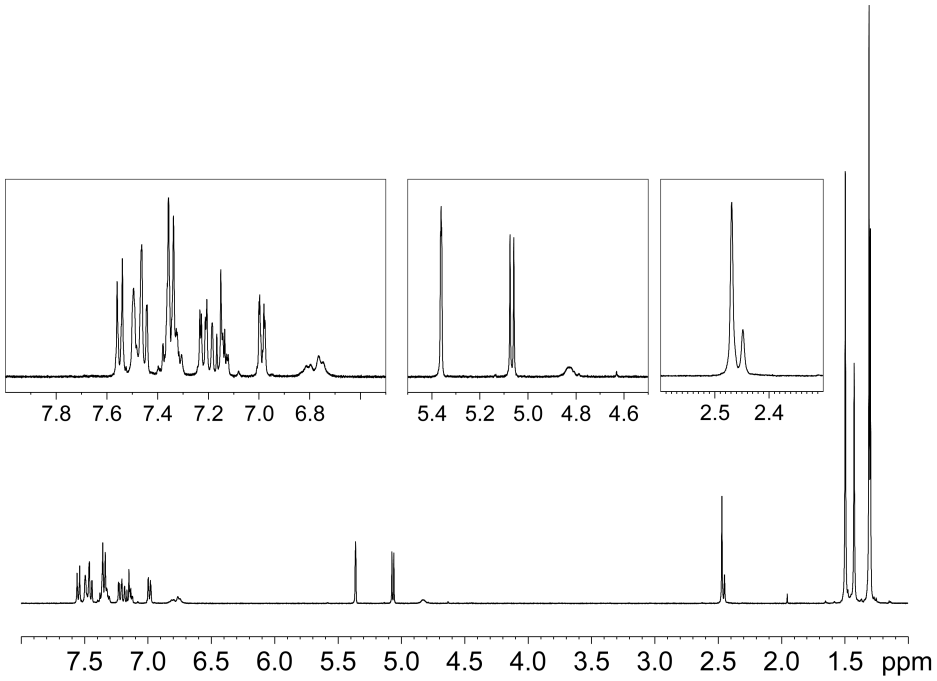

Figure S11. ^{1}H NMR spectrum obtained after mixing **1**TFA with 1.5 equivalents of **3** in dry methylene chloride-d_2 at 233K showing the presence of both free and coordinated allene.

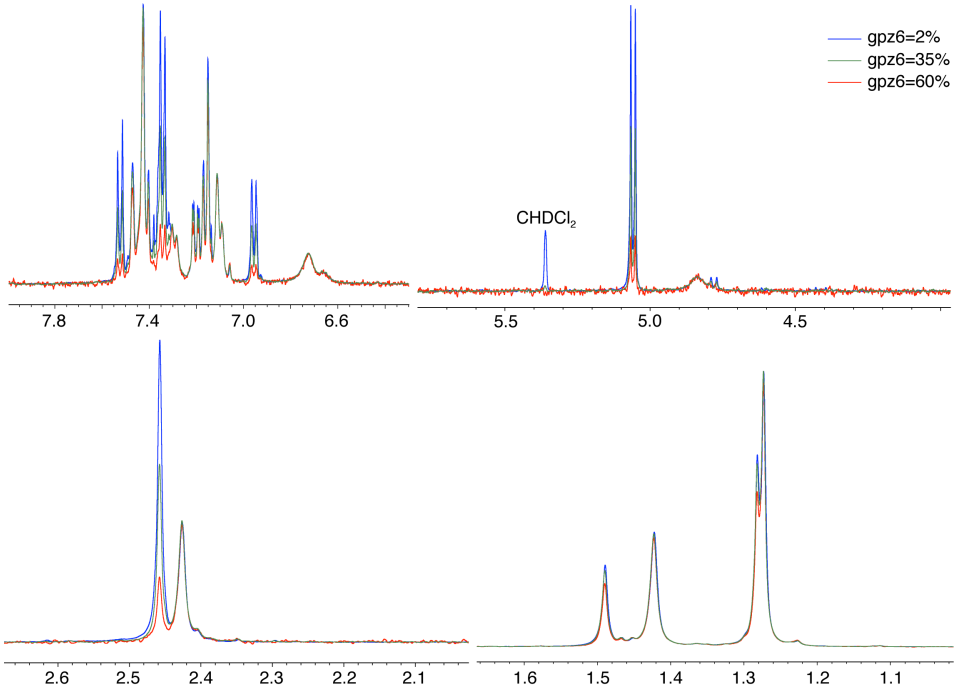

Figure S12. Four sections of ^{1}H PGSE NMR spectra obtained with 3 different gradient strengths of a mixture containing **1**TFA with 1.5 equivalents of **3** in dry methylene chloride-d_2 at 233K. Intensities of spectra were scaled to show the similar diffusion behaviour between coordinated **3** and $(RO)_3P$ resonances at δ_H=1.42 and 1.27 ppm.

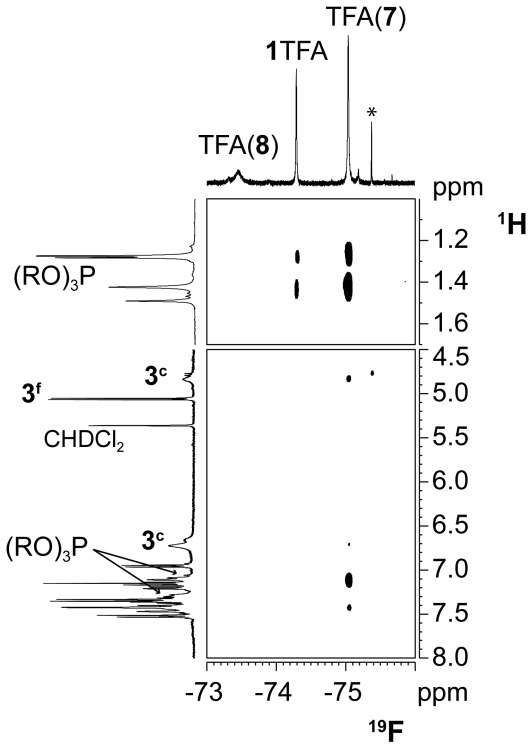

Figure S13. ^{19}F,^{1}H HOESY NMR spectrum of a mixture of **1**TFA and 1.5 equivalents of **3** in dry methylene chloride-d_2 at 233K. Asterisk denotes traces of **5** (see Scheme S2).

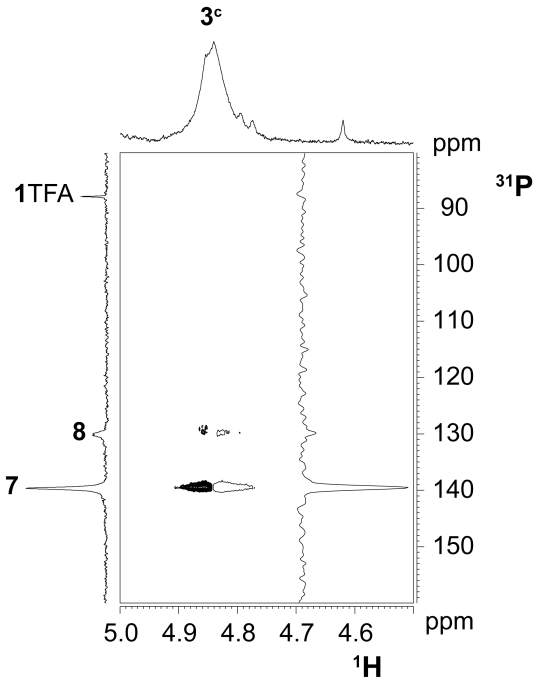

Figure S14. A section of the $^{1}H,^{31}P$ phase sensitive HMBC NMR spectrum of a mixture of **1**TFA and 8 equivalents of **3** in dry methylene chloride-d_2 at 233K.

2.4 1OTf + 3

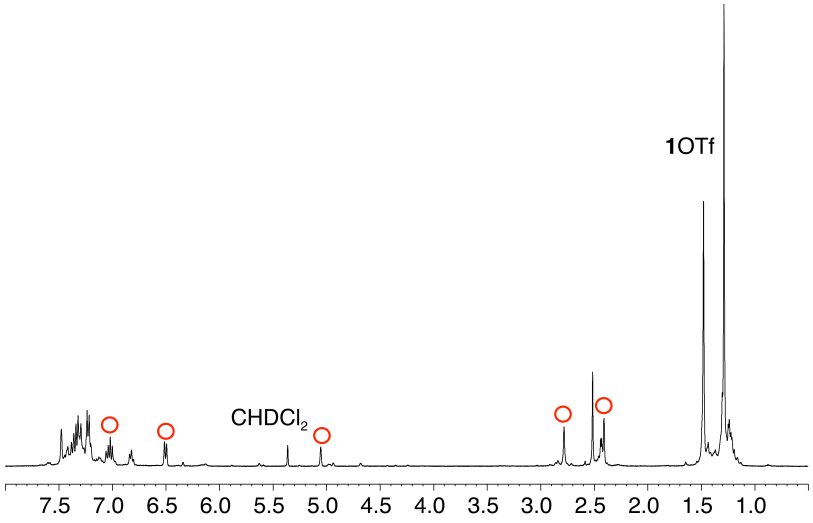

Figure S15. ^{1}H NMR spectrum obtained upon mixing **1**OTf with **2** equivalents of **3** in dry methylene chloride-d_2. Red circles denote main resonances of disubstituted cyclobutane obtained as side product.

3. In situ NMR catalytic experiments

Samples for kinetic NMR studies were prepared by loading the suitable amount of **2** and **3** within a screw cap NMR tube and by injecting 0.6 ml of catalyst solution in anhydrous methylene chloride-d_2. The reaction was monitored by ^{1}H and $^{31}P\{^{1}H\}$ NMR spectroscopies over the period of 12 hours at 298 K. Concentration *versus* time plots were obtained from integration of NMR spectra and fitted by means of COPASI software package, by imposing a two independent second order reaction model as follows:

2 + **3** → **4a**
2 + **3** → **4b**

$$\frac{d[2]}{dt} = -k_{4a}[2][3] - k_{4b}[2][3]$$
$$\frac{d[3]}{dt} = -k_{4a}[2][3] - k_{4b}[2][3]$$
$$\frac{d[4a]}{dt} = k_{4a}[2][3]$$
$$\frac{d[4b]}{dt} = k_{4b}[2][3]$$

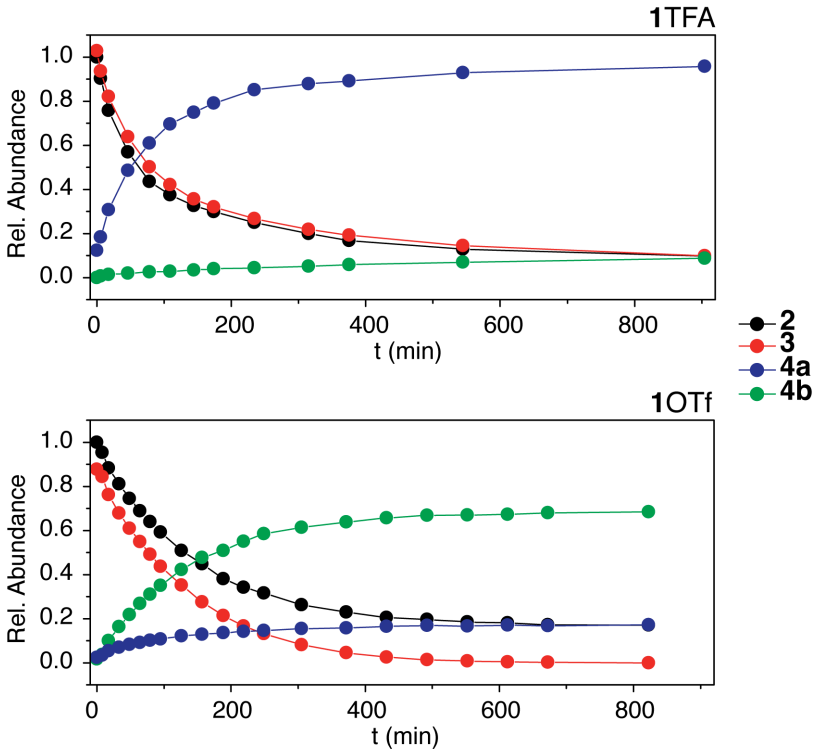

Figure S16. Kinetic profiles for dearomatization of **2** with **3** catalyzed by **1**TFA (top) and **1**OTf (bottom) in methylene chloride–d_2 at 298K.

3.1 1TFA

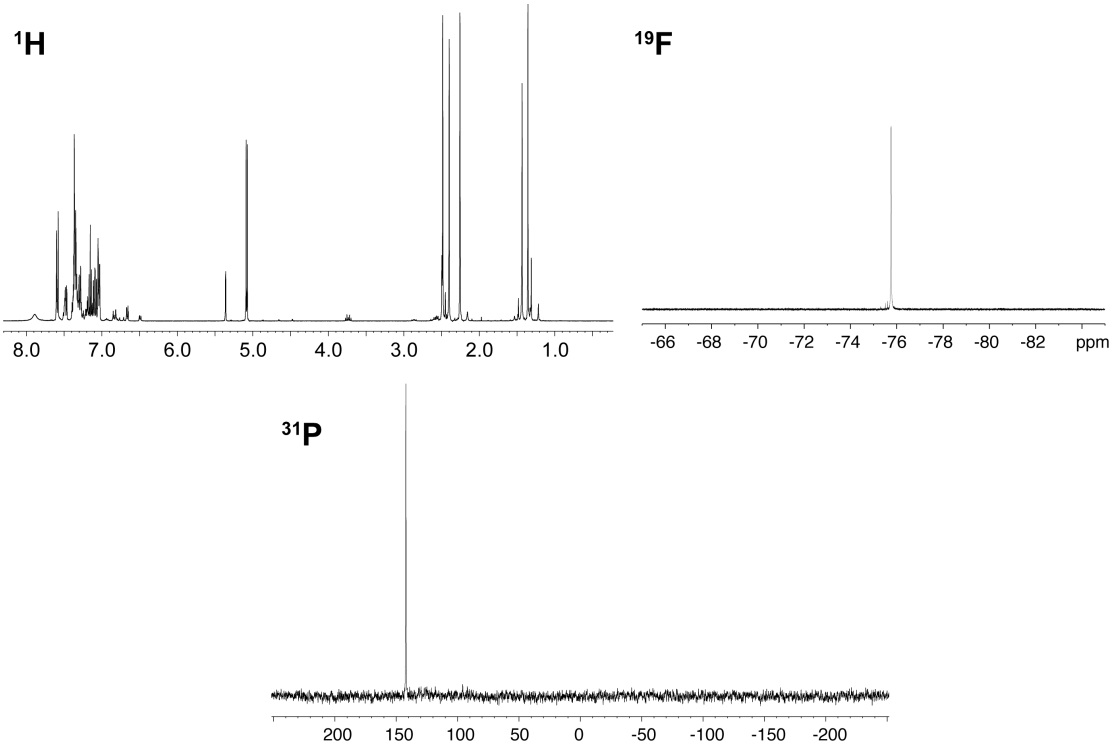

Figure S17. ^{1}H, ^{19}F and $^{31}P\{^{1}H\}$ NMR spectra obtained upon mixing **2**, **3** and **1**TFA (8% mol) in anhydrous methylene chloride-d_2 at 298K.

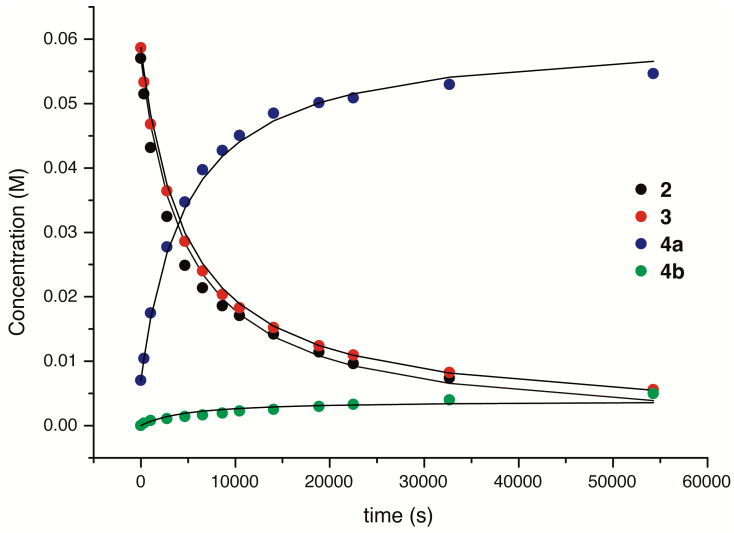

Figure S18. Concentration *versus* time plot for dearomatization reaction of **2** with **3** catalysed by **1**TFA. Mathematical fitting by imposing a two independent reaction model (black lines) gave a k_{4a}=3.4x10^{-3} M^{-1} s^{-1} and k_{4b}=2.5x10^{-4} M^{-1} s^{-1}.

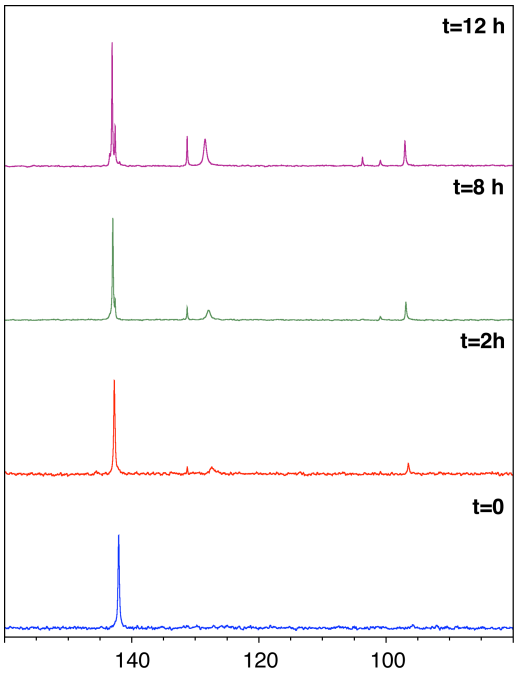

Figure S19. Evolution of $^{31}P\{^{1}H\}$ NMR spectrum with time of the reaction mixture during dearomatization reaction of **2** with **3** catalysed by **1**TFA.

3.1 1OTf

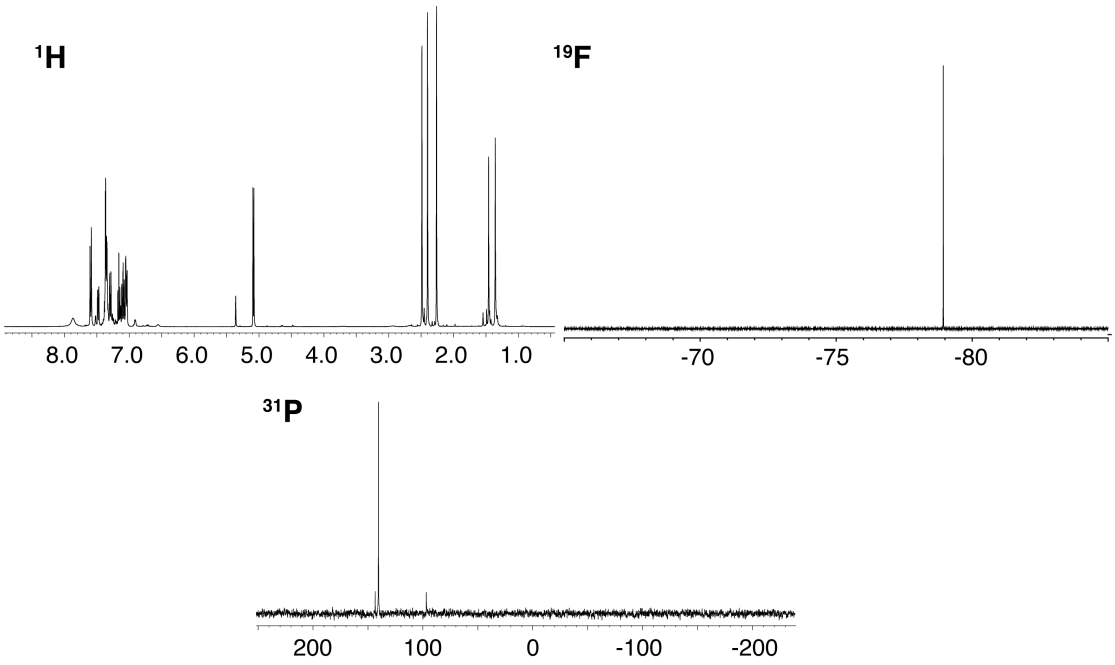

Figure S20. ^{1}H, ^{19}F and $^{31}P\{^{1}H\}$ NMR spectra obtained upon mixing **2**, **3** and **1**OTf (5% mol) in anhydrous methylene chloride-d_2 at 298K.

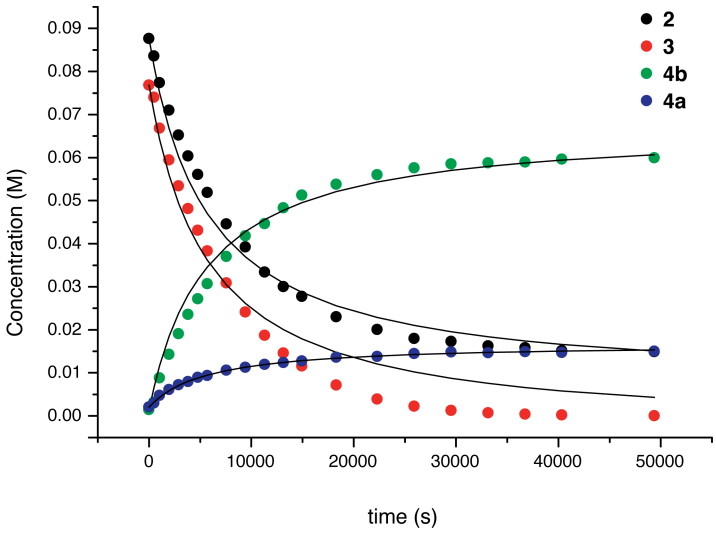

Figure S21. Concentration *versus* time plot for dearomatization reaction of **2** with **3** catalysed by **1**OTf. Mathematical fitting by imposing a two independent reaction model (black lines) gave a k_{4a}=3.9x10^{-4} M^{-1} s^{-1} and k_{4b}=1.7x10^{-3} M^{-1} s^{-1}.

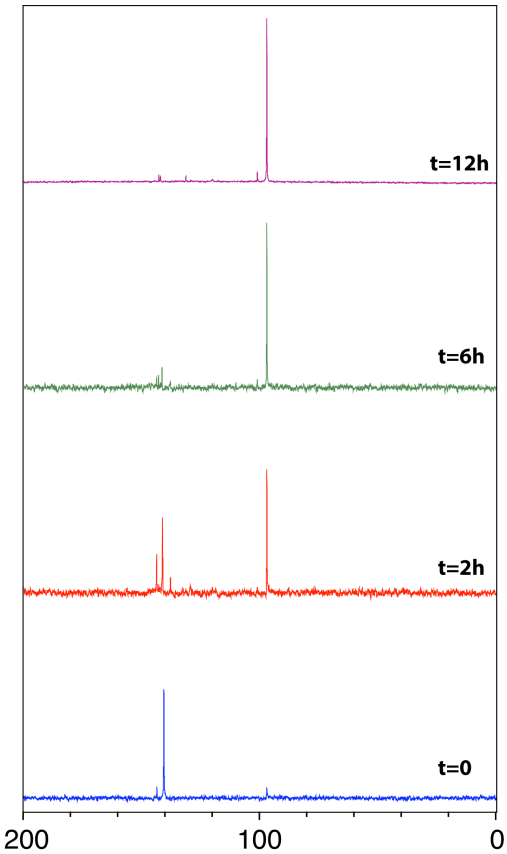

Figure S22. Evolution of ^{31}P{^{1}H} NMR spectrum with time of the reaction mixture during dearomatization reaction of **2** with **3** catalysed by **1**OTf.

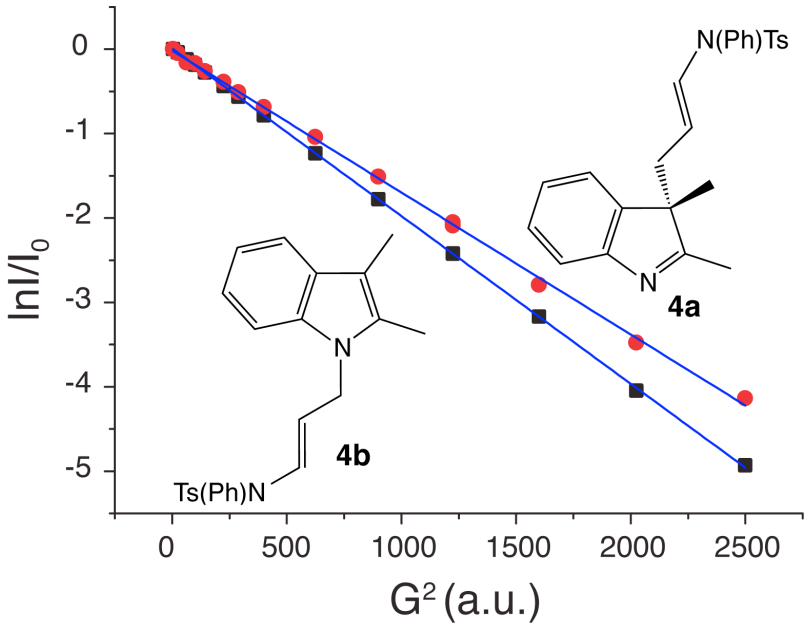

Figure S23. lnI/I_0 versus G^2 plot obtained by means of ^{1}H PGSE NMR experiments on the reaction mixture deriving from dearomatization of **2** catalysed by **1**OTf.

PGSE NMR CALCULATIONS:

$$\frac{slope(4b)}{slope(4a)} = \frac{1.99 \cdot 10^{-3}}{1.68 \cdot 10^{-3}} = 1.185$$

Given that the slope ratio is directly proportional to the self-diffusion coefficients ratio and inversely proportional to the hydrodynamic radii ratio, it can be derived that

$$\frac{D_t(4b)}{D_t(4a)} = \frac{r_H(4a)}{r_H(4b)} = 1.185$$

Therefore, the experimental **4a**/**4b** hydrodynamic volume ratio is $(1.185)^3$=1.662

Assuming the Van der Waals volumes of **4a** and **1**OTf equal to 370 and 730 Å^3, respectively, and considering that, at the end of the reaction, **3** equivalents of **4a** are present, if all $(RO)_3PAu^+$ cation is bound to **4a** it should be observed that:

$$V_{4a}{}^* = (x_{free} V_{4a}) + ((1 - x_{free}) V_{Au-4a}) = (0.67 \cdot 370) + (0.33 \cdot 1100) = 610.9 A^3$$

In perfect agreement with the experimental data, $\frac{V_{4a}{}^*}{V_{4b}} = \frac{610.9}{370} = 1.651$

References

(1) Zalesskiy, S. S.; Sedykh, A. E.; Kashin, A. S.; Ananikov, V. P. *J. Am. Chem. Soc.* **2013**, *135*, 3550–3559.
(2) Jia, M.; Cera, G.; Perrotta, D.; Monari, M.; Bandini, M. *Chem. Eur. J.* **2014**, *20*, 9875–9878.
(3) Wagner, R.; Berger, S. *J. Magn. Reson. Ser. A* **1996**, *123*, 119–121.
(4) Lix, B.; Sönnichsen, F. D.; Sykes, B. D. *J. Magn. Reson. Ser. A* **1996**, *121*, 83–87.
(5) Macchioni, A.; Ciancaleoni, G.; Zuccaccia, C.; Zuccaccia, D. *Chem. Soc. Rev.* **2008**, *37*, 479–489.